Van Hove singularities in doped twisted graphene bilayers studied by scanning tunneling spectroscopy

V. Cherkez,[1,2,3] G. Trambly de Laissardière,[4] P. Mallet,[1,2] and J.-Y. Veuillen[1,2,*]

[1]*Université Grenoble Alpes, Institut Neel, F-38042 Grenoble, France*

[2]*CNRS, Institut Neel, F-38042 Grenoble, France*

[3]*LNCMI, CNRS-UJF-UPS-INSA, 25 rue des Martyrs, F-38042 Grenoble, France*

[4]*Laboratoire de Physique Théorique et Modélisation, CNRS, Université de Cergy-Pontoise, F-95302 Cergy-Pontoise, France*

(Received 28 January 2015; published 24 April 2015)

The effect of electron doping on the van Hove singularities (vHs) which develop in twisted graphene bilayers (tBLs) is studied for a broad range of rotation angles θ ($1.5^\circ < \theta < 15^\circ$) by means of scanning tunneling microscopy and spectroscopy. Bilayer and trilayer graphene islands were grown on the 6H-SiC(000-1) (3×3) surface, which results in tBLs doped in the 10^{12} cm^{-2} range by charge transfer from the substrate. For large angles, doping manifests in a strong asymmetry of the positions of the upper (in empty states) and lower (in occupied states) vHs with respect to the Fermi level. The splitting of these vHs energies is found essentially independent of doping for the whole range of θ values, but the center of theses vHs shifts towards negative energies with increasing electron doping. Consequently, the upper vHs crosses the Fermi level for smaller angles (around 3°). The analysis of the data performed using tight-binding calculations and simple electrostatic considerations shows that the interlayer bias remains small (< 100 mV) for the doping level resulting from the interfacial charge transfer ($\simeq 5 \times 10^{12}$ cm^{-2}).

DOI: 10.1103/PhysRevB.91.155428 PACS number(s): 73.22.Pr, 61.48.Gh, 68.37.Ef, 73.20.At

I. INTRODUCTION

Twisted bilayers form a class of graphene-based materials whose low-energy electronic structure can be controlled by a geometric parameter, namely, by the rotation angle θ between the graphene layers. For undoped (neutral) systems, this property has been established by a number of theoretical [1–11] and experimental studies [12–18]. For large angles ($\theta > 10^\circ$), the layers are electronically decoupled, and the low-energy band structure looks like a simple superposition of the Dirac cones of the individual graphene planes [3–5,9,12,19]. For smaller angles, the interlayer interaction causes a decrease in the Fermi velocity [1,5,9,15] of either cone. Moreover, a pair of logarithmic divergences in the density of states (DOS) called van Hove singularities (vHs), related to a saddle point in the band structure, develop within 1 eV from the Fermi level [5,11,13,14,20]. Their energies are almost symmetric with respect to the Fermi level and decrease with θ [5,11,14,16,17,20]. For even smaller angles ($\theta < 1$ to 2°), flat bands appear at low energy [6,7,9], the vHs tend to localize in AA-stacked areas [5,14], and additional low-energy DOS features related to confinement appear [6].

The twist-induced changes in the band structure should be reflected in the physical properties of the bilayers. A rich physics is anticipated in magnetotransport experiments provided the Fermi level E_F can be brought in the vicinity or above the vHs [11,21–24], although it has not yet been revealed by the experiments reported so far [25–29]. Among the expected effects are the change in the degeneracy and the energy dependance of the Landau levels on either side of the vHs [21,22] and the emergence of a fractal energy spectrum (Hofstadter's butterfly) in strong magnetic fields for low rotation angles [11,23,24]. This would result in a change in the sign of the Hall conductivity when E_F crosses the vHs energy and eventually (at high field and for small θ values) in a nonmonotonic behavior of this quantity with increasing doping [11].

Structures in the optical conductivity induced by the presence of the vHs have been reported in a wide energy range depending on the value of θ [30–32] as expected from theoretical studies [33,34]. Calculations also predict that doping could markedly influence the optical properties when E_F reaches the vHs [33,35], e.g., by inducing an additional sharp absorption line related to an optical transition across the partial gap due to interlayer coupling. Owing to the variety of original properties expected upon doping, it is important to determine in a direct way the influence of this parameter on the low-energy electronic structure of the twisted graphene layers. This is especially interesting for the doping levels which are accessible using a backgate, typically a few 10^{12} cm^{-2} from Refs. [36–39], to determine for instance at which angle one vHs crosses E_F for a given charge. This would additionally allow the experimental investigation of the many-body instabilities expected in this configuration [40].

In this paper we perform an analysis by scanning tunneling microscopy (STM) and scanning tunneling spectroscopy (STS), complemented by tight-binding (TB) calculations, of the density of states of electron-doped twisted graphene bilayers in a wide range of angles ($1.5^\circ < \theta < 15^\circ$). We have investigated the electronic structure of twisted bilayers (tBLs) doped by charge transfer from the 6H-SiC(000-1) substrate (SiC-C face). Spectroscopic studies [41–44] have revealed that few-layer graphene films grown on this substrate are electron doped in the 10^{12} cm^{-2} range. The doping level is larger for the plane closest to the substrate (first plane) and decreases for consecutive layers as expected [45–47]. It becomes quite small for the fifth layer from the interface [42,43]. Thus bilayer and trilayer graphene islands on the SiC-C face should present a sizable layer-dependent doping level. This charge

*jean-yves.veuillen@neel.cnrs.fr

distribution results in a different electric potential on each graphene plane [45–47], which shifts the electronic energy levels (e.g., the Dirac points for electronically uncoupled planes [47]) of the layers accordingly. We find that the vHs cross the Fermi level for $\theta \simeq 3^\circ$ for bilayer islands with no change in the vHs splitting compared to the neutral case [17]. The layer-dependent doping results in a difference in the electrical potentials of the two layers on the order of 0.1 V at most as deduced from a simple model supported by experimental observations. Although weak, this difference should make the observation of topologically protected helical modes possible at sufficiently small angles [48].

II. EXPERIMENT

The sample has been prepared *in situ* by high-temperature graphitization of a clean 6H-SiC(000-1) (3×3) [in short SiC(3×3)] surface, following the recipe given in Refs. [49,50]. The temperature and annealing time were adjusted to get a sufficient density of bilayer and trilayer islands surrounded by uncovered portions of the bare SiC(3×3) surface. This morphology largely facilitates the identification of the number of graphene layers in the islands [20], which is otherwise somewhat ambiguous. As reported before [49,50], the substrate surface below the islands can show either SiC(3×3) or SiC(2×2) reconstructions. We focus there on bilayer and trilayer graphene islands on SiC(3×3) since the impact of this later reconstruction on the electronic properties of the first graphene layer is minimal [49,51,52], therefore it can be considered as genuine graphene. Owing to the discontinuous nature of the graphene film, STM and STS experiments were performed at room temperature to avoid artifacts, linked to the poor surface conductivity of the bare SiC(3×3) surface, which may occur at low sample temperature [53,54] (we have checked that our measurements were free of such artifacts, see Ref. [20]). Finally, the rotation angle θ between the twisted graphene layers was deduced from period P of the related (interlayer) moiré pattern (MP) in STM images [P (nm) $\simeq 14.1/\theta(^\circ)$] [55,56]. Notice that the interface between the first graphene layer and the SiC(3×3) surface also gives rise to an interface MP which remains clearly visible for bilayer islands (see Figs. 1 and 2). The characteristics of those interface MPs described in Ref. [51] allow differentiating them from the interlayer MP [20]. The conductance (dI/dV) STS spectra were obtained by numerically differentiating $I(V)$ curves recorded with an open feedback loop. The data were analyzed with the WSXM software [57].

III. RESULTS AND DISCUSSION

The effect of electron (n-type) doping on the electronic structure of a twisted graphene bilayer on SiC(3×3) is illustrated in Fig. 1(a) (a sketch of the interface structure is displayed at the bottom of the panel). This picture, which is approximately valid for a large rotation angle (say $\theta > 3^\circ$), is supported by our tight-binding calculations (see below). Without hybridization between the electronic states of the two graphene planes [uncoupled case, dotted lines in Fig. 1(a)] the Dirac cones of both layers (with Dirac points at K_1 and K_2) are shifted below the Fermi level by a different quantity owing

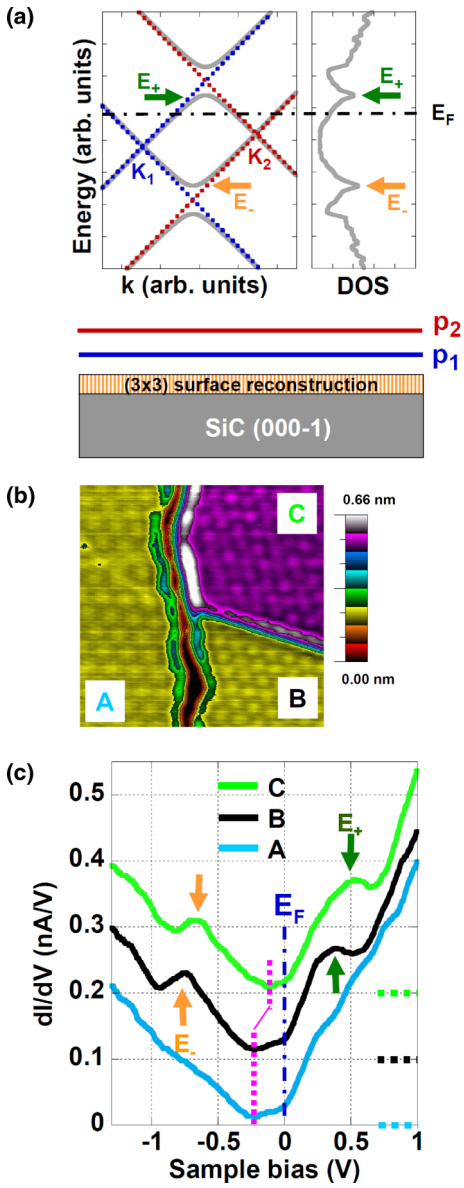

FIG. 1. (Color online) Influence of electron doping on the positions of the vHs. (a) Schematic of the electronic structure of a tBL doped by charge transfer from the 6H-SiC(000-1) (3×3) substrate. Bottom panel: side view of the sample structure. Top panel, left: band structure along a line connecting the Dirac points (located at K_1 and K_2) of the two rotated graphene layers. The dotted lines are the low-energy bands of the uncoupled layers (blue for p_1, red for p_2). The gray lines are the bands for the bilayer after switching on the electronic interaction. E_+ and E_- indicate the energies of the saddle points which result from this coupling. Top panel, right: total DOS for the coupled twisted bilayer. The saddle points give rise to vHs at E_+ and E_-. E_F indicates the Fermi level. For a doped tBL, E_+ and E_- are not symmetrical with respect to E_F. (b) STM image (32.3×32.3 nm^2, sample bias: -1.5 V) of an area with one bilayer island (zone A) with $\theta \simeq 14.0^\circ$ and a mixed bilayer (zone B)/trilayer (zone C) island with $\theta \simeq 6.0^\circ$. (c) STS spectra acquired on the three islands in (b). Stabilization bias/current: -1.5 V/0.2 nA. The curves have been shifted vertically for clarity (the origin of the conductance for each curve is indicated by the dotted line on the right). The green (orange) arrows indicate the positions of the upper (lower) vHs at E_+ (E_-).

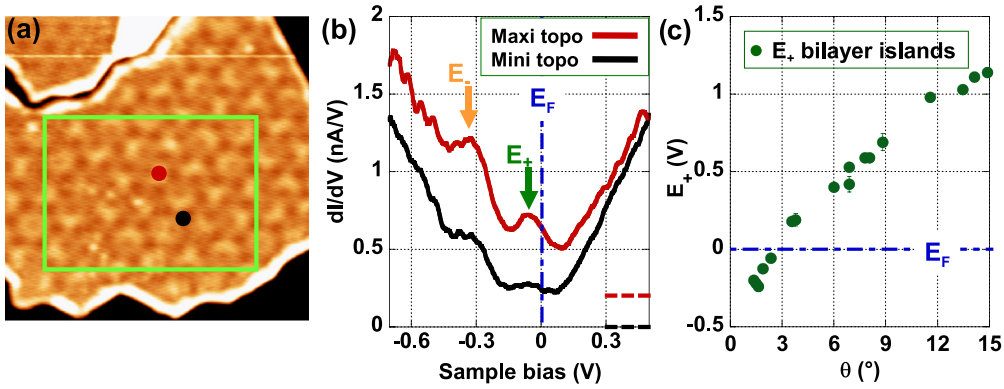

FIG. 2. (Color online) Position of the upper vHs relative to the Fermi level as a function of the rotation angle. (a) STM image (50×50 nm^2, sample bias: -2.0 V) of a bilayer island with $\theta = 2.3^\circ$ highlighted by the green square. Inside the square the red (black) point marks the position of a topographic maximum (minimum) of the interlayer moiré pattern. (b) Local STS spectra acquired at topographic maxima (red curve) and minima (black curve) of the bilayer island in (a). Stabilization bias/current: $+0.5$ V/0.3 nA. The curves have been shifted vertically for clarity (the origin of the conductance for each curve is indicated by the dotted line on the right). The green (orange) arrows indicate the positions of the upper (lower) vHs at E_+ (E_-). E_+ is located below the Fermi level E_F for this value of θ. (c) Energy E_+ (relative to E_F) of the upper vHs as a function of θ for 17 independent bilayer islands.

to different doping levels (equivalently: to different electric potentials) as shown in the left panel of Fig. 1(a). When hybridization is switched on, the band structure (gray lines) presents partial gaps at the crossing points of the uncoupled cones, which result in two vHs at energies E_+ (upper vHs) and E_- (lower vHs). The resulting total DOS (right panel) presents two peaks corresponding to those vHs. An obvious difference with the neutral (undoped) case [17] is that the vHs energies E_+ and E_- are no longer symmetrical with respect to the Fermi level E_F (this is $E_+ \neq -E_-$). This strong asymmetry is a hallmark for the bilayer doping, and it is expected to decrease with decreasing total charge in the tBL.

The experimental results shown in Fig. 1 support these considerations. Figure 1(b) shows an STM image of an area with two bilayer islands with different rotation angles (zone A: $\theta \simeq 14^\circ$, zone B: $\theta \simeq 6^\circ$) and a trilayer island (zone C) with a rotation angle $\theta \simeq 6^\circ$ between the surface layers [20]. Interleaved STS spectra (proportional to the local DOS) taken on those three zones are shown in Fig. 1(c). They show peaks (indicated by arrows) in zones B and C that we ascribe to the vHs of the surface (outermost) tBL since they are absent in zone A and thus are not tip artifacts. Peaks corresponding to the vHs are identified at higher energy in zone A. Interestingly, the energies of the upper and lower vHs are strongly asymmetrical with respect to E_F for both the bilayer and the trilayer islands, but the asymmetry is reduced for the later case as a consequence of a lower overall charge of the surface tBL. The data of Fig. 1 thus confirm that the vHs are still present for doped layers and that they shift downwards in energy with increasing electron doping.

As a first approach to the problem we can consider that the total charge of a tBL should not vary much with the rotation angle θ. If one considers first the mechanism for graphene doping based on electron transfer from donorlike states of the SiC(3×3) surface [58], the argument is that the transferred charge is the one required to build the interface dipole which serves to equalize the Fermi level of the substrate and of the bilayer upon contact [59]. Hence, provided that the work function of the tBL does not change much with θ (to our knowledge this dependence has not been measured) the interface dipole and thus the total transferred charge should remain approximately constant. The same conclusion is reached if one considers the other mechanism proposed in Ref. [58] and experimentally demonstrated in Ref. [60] where the doping arises from the spontaneous polarization in the hexagonal 6H-SiC substrate. This mechanism should effectively result in electron accumulation (doping in the 10^{12} cm^{-2} range) in a tBL layer on top of the SiC-C face considered there [58] in order to balance the polarization (pseudo) charge. However, since the spontaneous polarization is a property of the bulk substrate there is no obvious reason why the total charge of the tBL should depend on the interlayer rotation angle θ.

Now in the undoped (neutral) case the energy of the upper (lower) vHs decreases (increases) with respect to E_F for decreasing angles [17]. As a result one may anticipate from the data of Fig. 1(b) that for small enough θ values the energy of the upper vHs E_+ can be pushed below the Fermi level for a roughly constant doping level. This is indeed the case as shown in Fig. 2. The STM image of Fig. 2(a) shows a bilayer island with a twist angle of $\theta \simeq 2.3^\circ$ (inside the green rectangle). STS spectra on topographic maxima (minima) of the interlayer MP indicated by red (black) dots in Fig. 2(a) are shown in Fig. 2(b). They show peaks, indicated by arrows, which correspond to the vHs of the twisted layers. These structures are again absent in spectra (not shown) taken with the same tip on the twisted bilayer in the upper left corner of Fig. 2(b), which has a larger value of $\theta \simeq 13.4^\circ$. In accordance with the results obtained for neutral tBL [6,14,17] the amplitude of the vHs peaks becomes strongly modulated within the MP for such a small angle of $\theta \simeq 2.3^\circ$. This reinforces our interpretation of these peaks as due to the vHs, considering that our TB calculations also reproduce this modulation for doped bilayers. The important point is that the upper vHs is now located below the Fermi level, this is $E_+ < E_F$. The experimental variation in E_+ as a function of the rotation angle, measured by STS on different

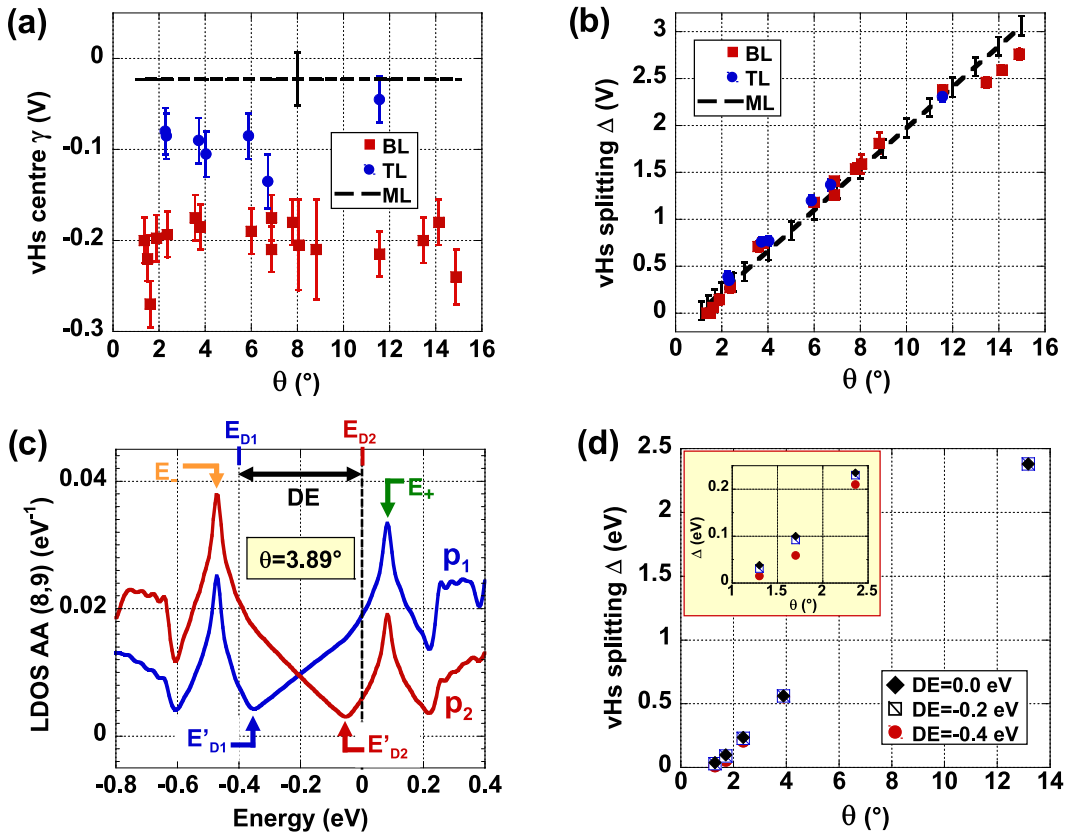

FIG. 3. (Color online) Center γ and splitting Δ of the upper and lower vHs for a doped tBL as a function of θ. (a) Experimental value of γ for bilayer (red squares) and trilayer (blue dots) islands. The black dashed lines shows the average value for an almost neutral multilayer (ML), adapted from Ref. [17]. (b) Experimental value of Δ for bilayer (red squares) and trilayer (blue dots) islands. The black dashed lines shows the mean (fitted) value for an almost neutral ML, adapted from Ref. [17]. (c) Computed local DOS (LDOS) in an AA-stacked region for a twisted bilayer with $\theta = 3.89°$ and a difference in on-site energies $DE = -0.4$ eV between the two layers. Blue line: interface plane [p_1 in Fig. 1(a)] and red line: surface plane [p_2 in Fig. 1(b)]. E'_{D1} and E'_{D2}: positions of the (renormalized) Dirac points of the two planes for the coupled bilayer. E_{D1} and E_{D2}: positions of the (bare) Dirac points of the two uncoupled layers. E_+ and E_- indicate the upper and lower vHs, respectively. (d) Computed value of the vHs splitting for different values of DE as a function of θ. Inset: zoomed-in view on the small-angle region.

bilayer islands, is given in Fig. 2(c). It shows that the upper vHs can be brought close to the Fermi level for $\theta \simeq 3°$. This would give the opportunity to investigate in this system the amazing many-body effects predicted theoretically [40].

We have analyzed the vHs energies E_+ and E_- on 17 (7) independent twisted bilayer (trilayer) islands, covering a wide range of rotation angles ($1.5° < \theta < 15°$). The experimental values of the center $\gamma = (E_+ + E_-)/2$ and of the splitting $\Delta = (E_+ - E_-)$ of the vHs are displayed in Figs. 3(a) and 3(b), respectively. For comparison, the same quantities measured on a thicker—and thus almost neutral—ML grown on the same substrate [17] are shown as dashed black lines in Figs. 3(a) and 3(b). The shift in γ [Fig. 3(a)] towards more negative values for decreasing sample thickness reflects the larger doping of the two outermost (surface) twisted graphene planes. For a given thickness, the value of γ remains essentially constant as a function of the rotation angle θ. The average values of γ are as follows: $\gamma = -0.02 \pm 0.03$ eV for the thick multilayer, $\gamma = -0.20 \pm 0.03$ eV for the bilayer islands, and $\gamma = -0.09 \pm 0.03$ eV for the trilayer ones. Figure 3(b) shows that the vHs splitting Δ has essentially the same quasilinear variation with θ for any sample thickness. Δ is therefore independent of the doping level of the tBL and on the related interlayer potential difference. This fact suggests that the vHs splitting contains little information on the charge distribution among graphene layers, which is only reflected in the value of γ.

We have performed TB calculations to gain more insight into the electronic structure of doped twisted bilayers. Numerical simulations addressing this issue have already been published [1,35,48,61,62], but they were limited to a restricted set of angles, they used different computational techniques, and they mostly considered the band structure and not the LDOS features as in the STS measurements. When comparison is possible our results are consistent with these previous works. We have investigated a range of angles ($1.3° < \theta < 13.2°$) corresponding to the experimental one using the TB approach described in Refs. [5,6] and the set of hopping parameters which reproduces the experimental data for thick layers [17]. A difference in the electric potential of the two graphene planes was enforced by setting a different on-site energy ϵ^0 for the C $2p_z$ orbital on planes p_1 ($\epsilon^0 = DE < 0$) and p_2 ($\epsilon^0 = 0$ eV). An (overall) additional doping of the layer can subsequently

be mimicked by simply shifting the energy scale of the LDOS curves by a constant value, assuming the Fermi level remains at zero energy as in the experiments.

We have computed both the total DOS of the bilayer and the local DOS in AA-stacked areas of either plane (which correspond to the topographic maxima of the MP [17,63], e.g., in Figs. 1 and 2). Figure 3(c) shows the AA LDOS on the two layers for $\theta = 3.89^\circ$ and $DE = -0.4$ eV. The peaks corresponding to the positive (at E_+) and negative (at E_-) vHs are indicated by arrows. In between these peaks there is a clear minimum for p_1 and p_2, at energies denoted E'_{D1} and E'_{D2}, that we ascribe to the (renormalized) Dirac points on each plane of the coupled tBL following previous band-structure calculations performed for the same angle [1,35,62]. Notice that these minima are slightly shifted with respect to the values expected without interlayer coupling, which would be $E_{D1} = DE$ and $E_{D2} = 0$ eV (indicated in the upper part of the figure) as also shown in Refs. [1,35,62]. This shift decreases for larger angles, becoming zero for $\theta > 13^\circ$ (see also Refs. [35,61]). This effect will be discussed in a separate paper [64]. For the moment we only consider the quantities which are pertinent for the analysis of the experimental data, this is the splitting Δ and the center γ of the vHs. Figure 3(d) shows that Δ is almost insensitive to the interlayer potential difference DE (especially for $DE = -0.2$ eV) for all angles, in accordance with previous reports [1,35,48,61,62]. This is in excellent agreement with our experimental findings for Δ [Fig. 3(a)]. Only for a restricted angular range ($\theta \simeq 1.7^\circ$) and for a large DE value ($DE = -0.4$ eV) do we observe a sizable difference in the computed vHs splitting as shown in the inset of Fig. 3(d). However, our estimate of the interlayer potential difference (see below) indicates that $DE = -0.4$ eV is a too large value ($DE = -0.2$ eV would be more realistic). Thus the calculations confirm that the vHs splitting is almost independent of doping as found experimentally.

The computed value of the vHs center $\gamma = (E_+ + E_-)/2$ for all values of DE and θ is almost equal to $(E'_{D1} + E'_{D2})/2$ as long as E'_{D1} and E'_{D2} can be defined [20] (this is for $\theta > 1.5^\circ$). This theoretical result is independent of any additional doping that one would introduce in the system by shifting the Fermi level since then all quantities (E_+, E_-, E'_{D1}, and E'_{D2}) would move accordingly. It is thus also consistent with previous works [1,35,61,62] where opposite potentials were enforced on the two layers in the calculations. Therefore the experimental value of γ also gives the average of the (renormalized) Dirac point energies of the tBL. From Fig. 3(b) we observe that this quantity is essentially independent of the rotation angle. For bilayer islands, the value we obtain for $\gamma \simeq (E'_{D1} + E'_{D2})/2 \simeq -0.20$ eV is consistent with the one reported in a recent angle-resolved photoemission spectroscopy study (-0.19 eV) for a nominally two-layer graphene sample grown on a SiC(3×3) surface [44] (see also Ref. [41]).

The value of the average Dirac point energy however does not give a detailed account of the charge distribution between the layers. For instance it does not provide *a priori* any indication on the value of the difference in the electric potential of the graphene planes. Nevertheless the value of γ alone should in principle be sufficient to recover the main features of this charge distribution (charge and potential on either plane) provided a self-consistent treatment of the problem is performed. Indeed, the charge on p_2 (surface plane) determines the interlayer potential difference U through Gauss theorem [45–47] (referring to our TB calculations $DE = -eU$, where $e = 1.6 \times 10^{-19}$ C). From this quantity a band-structure calculation of the biased twisted bilayer can be performed for a given value of θ. The energy of the Fermi level E_F of the bilayer is then the one which gives the correct value of the charge on plane p_2. This value of E_F in turns allows computing the charge on plane p_1 (interface plane). Although feasible in principle this procedure has to tackle the full complexity of the problem, including not only the change in the band structure of the bilayer with θ, but also with the interlayer bias U [1,62,65] (for instance it appears from Fig. 2 of Ref. [62] that the layer population of the low-energy bands change with U and in Fig. 3 of Ref. [65] that the excess charge on one layer strongly depends on θ for a given U). To our knowledge such self-consistent treatment has not been performed so far for twisted bilayers.

To get at least a qualitative idea of the charge/potential distribution from our γ value we have to resort to a simpler model which considers electronically decoupled layers as in Refs. [46,47]. This model should give realistic information in the case of large angles ($\theta > 10^\circ$), small doping, and small interlayer bias compared to the vHs splitting since in this situation the states close to the Dirac points of either layer are weakly perturbed by the interlayer coupling [1,3–5,9,19]. For an electron-doped system, using the notation: E_{D1} (E_{D2}) energy of the Dirac points of p_1 (p_2) with respect to the Fermi level E_F (energy reference at E_F), n_1 (n_2): density of electrons in p_1 (p_2) and U: value of the interlayer potential difference, one has

$$n_i = \frac{E_{Di}^2}{\pi(\hbar v_F)^2}, \quad i = 1,2, \tag{1}$$

from the band structure with v_F as the Fermi velocity in monolayer graphene,

$$U = \frac{en_2 d}{\epsilon}, \tag{2}$$

from the Gauss theorem with $\epsilon = \epsilon_r \epsilon_0$ as the dielectric constant of the medium and d as the interlayer distance.

Now, since $E_{D1} - E_{D2} = -eU$, we have

$$E_{D1} = E_{D2} - e\frac{ed}{\epsilon}\frac{E_{D2}^2}{\pi(\hbar v_F)^2}. \tag{3}$$

Hence,

$$\gamma = \frac{E_{D1} + E_{D2}}{2} = E_{D2} - \frac{e^2 d}{2\epsilon}\frac{E_{D2}^2}{\pi(\hbar v_F)^2}. \tag{4}$$

Therefore the knowledge of the mean value of the Dirac energies is sufficient to determine E_{D2} and thus the other quantities (U,n_1,n_2) in this electrostatic self-consistent treatment. A sketch of the variation in the quantities E_{D1}, E_{D2}, U, n_1, and n_2 as a function of γ is given in the Supplemental Material [20] for the case of $\epsilon_r = 1$ and $v_F = 1.1 \times 10^6$ m/s [17,44]. Notice that this simple model which only considers the charges/potentials within the two graphene layers should apply whatever the mechanism of the bilayer doping: charge transfer from or spontaneous polarization of the substrate. Only the origin of the (pseudo)

positive charge counterbalancing the negative bilayer one will be different. In our case, for large angles the value $\gamma = (E_{D1} + E_{D2})/2 = (E'_{D1} + E'_{D2})/2 = -0.20$ eV applies for bilayer islands. The model thus gives: $E_{D1} = -0.25$, $E_{D2} = -0.16$, $E_{D1} - E_{D2} = -0.09$ eV, $n_1 = 3.8 \times 10^{12}$, $n_2 = 1.5 \times 10^{12}$ cm^{-2}, and a total charge of $n_1 + n_2 = 5.3 \times 10^{12}$ cm^{-2}. Considering the more realistic situation $\epsilon_r > 1$ reduces $|E_{D1} - E_{D2}|$ (in absolute value) but leaves $n_1 + n_2$ almost unaffected [20]. This total charge is on the order of what can be obtained through gate doping on an oxidized Si substrate [36–39], and thus our findings for the position of the vHs with respect to the Fermi level as a function of θ [Fig. 2(c)] should also apply to this situation.

One result of our simple model is that the difference in the energies of the Dirac point of the two (uncoupled) layers (i.e., $-eU$ in this model) is rather small: -0.09 eV. An indication that this is indeed the case is given in Fig. 1(c). At low bias, apart from the ubiquitous minimum at zero bias which is commonly observed in graphene samples for any doping (see, e.g., Refs. [66,67]), we observe a second minimum indicated by a pink dotted line. It is located at the same energy for bilayer islands A and B and shifts towards zero bias for the trilayer island. We believe that this minimum is related to the renormalized Dirac point E'_{D2} of the surface layer p_2. In principle for large enough angles there is a broad and flat minimum between the Dirac points E'_{D1} and E'_{D2} in the total DOS (see, e.g., the right panel of Fig. 1(a) and Ref. [48]), but in STS we mostly probe the LDOS of the surface layer p_2 which indeed presents a minimum at E'_{D2}, see Fig. 3(c). The TB calculations show that the difference in energy between E'_{D2} and the center of the vHs γ is roughly on the order of $U/2$ (i.e., $-DE/2$ in TB calculations) for large enough angles ($\theta > 3.5°$), see, e.g., Fig. 3(c) and Supplemental Material [20]. Measurements of the position of the second minimum for $\theta > 3.5°$, although not very accurate, give an average value of $E'_{D2} = -0.19 \pm 0.04$ eV for bilayer islands. This is close to the average value of $\gamma(-0.20 \pm 0.03$ eV) for these islands, which confirms that the interlayer potential difference U is indeed small. We believe that this result should be rather general, whatever the interlayer coupling. Actually, a self-consistent study [68] of the variation in U with the total charge in an AB-stacked, and therefore strongly coupled, bilayer has established that for a total charge of $n_1 + n_2 \simeq 5.0 \times 10^{12}$ cm^{-2} the value of eU is on the order of 0.07 eV, similar to the one we get for uncoupled layers.

As a final remark, we would like to comment on the value of the total charge transferred on the bilayer islands as a function of θ. We have assumed at the beginning that this quantity should be rather constant. This would seem to be consistent with the observation that the average energy of the (renormalized) Dirac points $(E'_{D1} + E'_{D2})/2 \simeq \gamma$ does not vary much with θ [Fig. 3(b) on the condition that the band structure of the tBL in the vicinity of E_F will also remain unchanged. We see however in Fig. 2(c) that with a decreasing angle the Fermi level goes through energy values where the DOS strongly departs from one of the almost uncoupled layers, which corresponds to large angles. Namely, E_F crosses the vHs for $\theta \simeq 3°$. One may thus suspect that around this value the total charge varies rapidly with θ for a constant value of γ. In the absence of detailed self-consistent calculations this remains however speculative.

IV. CONCLUSION

We have studied the influence of electron doping on the electronic structure of twisted graphene bilayers for rotation angles between 1.5° and 15°. The doping level which results from charge transfer from the SiC substrate ($\simeq 5 \times 10^{12}$ cm^{-2}) is comparable to the one achievable by electrostatic gating, thus our findings should also apply to this situation. The upper van Hove singularity, which is located above E_F for the neutral samples is brought below E_F for doped tBLs with $\theta < 3°$. Significant changes in the optical or magnetotransport properties of the sample are expected in this regime. Experiments show that the splitting of the vHs does not change with doping, in agreement with tight-binding calculations. Finally, a simple modeling of the data indicates that the difference in the electric potentials of the two graphene layers remains small (<100 mV) for the charge transfer achieved in our samples.

ACKNOWLEDGMENTS

This work was supported by the European Union FP7 "Graphene Flagship" program (Grant No. 604391) and by CNRS PICS (Grant No. 6182). We thank L. Magaud, D. Mayou, I. Brihuega, F. Ynduráin, and J. M. Gómez-Rodríguez for helpful comments and discussions.

[1] J. M. B. Lopes dos Santos, N. M. R. Peres, and A. H. Castro Neto, Phys. Rev. Lett. **99**, 256802 (2007).
[2] J. M. B. Lopes dos Santos, N. M. R. Peres, and A. H. Castro Neto, Phys. Rev. B **86**, 155449 (2012).
[3] S. Latil, V. Meunier, and L. Henrard, Phys. Rev. B **76**, 201402(R) (2007).
[4] S. Shallcross, S. Sharma, E. Kandelaki, and O. A. Pankratov, Phys. Rev. B **81**, 165105 (2010).
[5] G. Trambly de Laissardière, D. Mayou, and L. Magaud, Nano Lett. **10**, 804 (2010).
[6] G. Trambly de Laissardière, D. Mayou, and L. Magaud, Phys. Rev. B **86**, 125413 (2012).
[7] R. Bistritzer and A. H. MacDonald, Proc. Natl. Acad. Sci. USA **108**, 12233 (2011).
[8] P. San-Jose, J. González, and F. Guinea, Phys. Rev. Lett. **108**, 216802 (2012).
[9] E. Suárez Morell, J. D. Correa, P. Vargas, M. Pacheco, and Z. Barticevic, Phys. Rev. B **82**, 121407(R) (2010).
[10] E. J. Mele, Phys. Rev. B **84**, 235439 (2011).
[11] P. Moon and M. Koshino, Phys. Rev. B **85**, 195458 (2012).
[12] M. Sprinkle, D. Siegel, Y. Hu, J. Hicks, A. Tejeda, A. Taleb-Ibrahimi, P. Le Fèvre, F. Bertran, S. Vizzini, H. Enriquez, S. Chiang, P. Soukiassian, C. Berger, W. A. de Heer, A.

Lanzara, and E. H. Conrad, Phys. Rev. Lett. **103**, 226803 (2009).
[13] T. Ohta, J. T. Robinson, P. J. Feibelman, A. Bostwick, E. Rotenberg, and T. E. Beechem, Phys. Rev. Lett. **109**, 186807 (2012).
[14] G. Li, A. Luican, J. M. B. Lopez dos Santos, A. H. Castro Neto, A. Reina, J. Kong, and E. Y. Andrei, Nat. Phys. **6**, 109 (2010).
[15] A. Luican, G. Li, A. Reina, J. Kong, R. R. Nair, K. S. Novoselov, A. K. Geim, and E. Y. Andrei, Phys. Rev. Lett. **106**, 126802 (2011).
[16] W. Yan, M. Liu, R.-F. Dou, L. Meng, L. Feng, Z.-D. Chu, Y. Zhang, Z. Liu, J.-C. Nie, and L. He, Phys. Rev. Lett. **109**, 126801 (2012).
[17] I. Brihuega, P. Mallet, H. González-Herrero, G. Trambly de Laissardière, M. M. Ugeda, L. Magaud, J. M. Gómez-Rodríguez, F. Ynduráin, and J.-Y. Veuillen, Phys. Rev. Lett. **109**, 196802 (2012).
[18] X. Zhang and H. Luo, Appl. Phys. Lett. **103**, 231602 (2013).
[19] J. Hass, F. Varchon, J. E. Millán-Otoya, M. Sprinkle, N. Sharma, W. A. de Heer, C. Berger, P. N. First, L. Magaud, and E. H. Conrad, Phys. Rev. Lett. **100**, 125504 (2008).
[20] See Supplemental Material at http://link.aps.org/supplemental/10.1103/PhysRevB.91.155428 for a basic description of the electronic interlayer coupling, for the bilayers/trilayers identification procedure, for the influence of stabilization parameters of STS spectra, for additional results of the tight-binding calculations, and for plots of the electrostatic model.
[21] M.-Y. Choi, Y.-H. Hyun, and Y. Kim, Phys. Rev. B **84**, 195437 (2011).
[22] R. de Gail, M. O. Goerbig, F. Guinea, G. Montambaux, and A. H. Castro Neto, Phys. Rev. B **84**, 045436 (2011).
[23] R. Bistritzer and A. H. MacDonald, Phys. Rev. B **84**, 035440 (2011).
[24] Z. F. Wang, F. Liu, and M. Y. Chou, Nano Lett. **12**, 3833 (2012).
[25] D. S. Lee, C. Riedl, T. Beringer, A. H. Castro Neto, K. von Klitzing, U. Starke, and J. H. Smet, Phys. Rev. Lett. **107**, 216602 (2011).
[26] D.-H. Chae, D. Zhang, X. Huang, and K. von Klitzing, Nano Lett. **12**, 3905 (2012).
[27] J. D. Sanchez-Yamagishi, T. Taychatanapat, K. Watanabe, T. Taniguchi, A. Yacoby, and P. Jarillo-Herrero, Phys. Rev. Lett. **108**, 076601 (2012).
[28] B. Fallahazad, Y. Hao, K. Lee, S. Kim, R. S. Ruoff, and E. Tutuc, Phys. Rev. B **85**, 201408(R) (2012).
[29] J.-J. Chen, J. Meng, D.-P. Yu, and Z.-M. Liao, Sci. Rep. **4**, 5065 (2014).
[30] X. Zou *et al.*, Phys. Rev. Lett. **110**, 067401 (2013).
[31] R. W. Havener, Y. Liang, L. Brown, L. Yang, and J. Park, Nano Lett. **14**, 3353 (2014).
[32] J. T. Robinson, S. W. Schmucker, C. B. Diaconescu, J. P. Long, J. C. Culbertson, T. Ohta, A. L. Friedman, and T. E. Beechem, ACS Nano **7**, 637 (2013).
[33] C. J. Tabert and E. J. Nicol, Phys. Rev. B **87**, 121402(R) (2013).
[34] P. Moon and M. Koshino, Phys. Rev. B **87**, 205404 (2013).
[35] P. Moon, Y.-W. Son, and M. Koshino, Phys. Rev. B **90**, 155427 (2014).
[36] H. Schmidt, T. Lüdtke, P. Barthold, E. McCann, V. I. Fal'ko, and R. J. Haug, Appl. Phys. Lett. **93**, 172108 (2008).
[37] H. Schmidt, T. Lüdtke, P. Barthold, and R. J. Haug, Phys. Rev. B **81**, 121403(R) (2010).
[38] K. Novoselov *et al.*, Science **306**, 666 (2004).
[39] L. A. Ponomarenko, R. V. Gorbachev, G. L. Yu, D. C. Elias, R. Jalil, A. A. Patel, A. Mishchenko, A. S. Mayorov, C. R. Woods, J. R. Wallbank, M. Mucha-Kruczynski, B. A. Piot, M. Potemski, I. V. Grigorieva, K. S. Novoselov, F. Guinea, V. I. Fal'ko, and A. K. Geim, Nature (London) **497**, 594 (2013).
[40] J. Gonzalez, Phys. Rev. B **88**, 125434 (2013).
[41] K. V. Emtsev, F. Speck, T. Seyller, L. Ley, and J. D. Riley, Phys. Rev. B **77**, 155303 (2008).
[42] D. Sun, C. Divin, C. Berger, W. A. de Heer, P. N. First, and T. B. Norris, Phys. Rev. Lett. **104**, 136802 (2010).
[43] J. Hicks, K. Shepperd, F. Wang, and E. H. Conrad, J. Phys. D: Appl. Phys. **45**, 154002 (2012).
[44] E. Moreau, S. Godey, X. Wallart, I. Razado-Colambo, J. Avila, M.-C. Asensio, and D. Vignaud, Phys. Rev. B **88**, 075406 (2013).
[45] F. Guinea, Phys. Rev. B **75**, 235433 (2007).
[46] H. Min, S. Adam, Y. J. Song, J. A. Stroscio, M. D. Stiles, and A. H. MacDonald, Phys. Rev. B **83**, 155430 (2011).
[47] M. A. Kuroda, J. Tersoff, and G. J. Martyna, Phys. Rev. Lett. **106**, 116804 (2011).
[48] P. San-Jose and E. Prada, Phys. Rev. B **88**, 121408 (2013).
[49] F. Hiebel, P. Mallet, F. Varchon, L. Magaud, and J.-Y. Veuillen, Phys. Rev. B **78**, 153412 (2008).
[50] F. Hiebel, L. Magaud, P. Mallet, and J.-Y. Veuillen, J. Phys. D: Appl. Phys. **45**, 154003 (2012).
[51] F. Hiebel, P. Mallet, L. Magaud, and J.-Y. Veuillen, Phys. Rev. B **80**, 235429 (2009).
[52] I. Deretzis and A. La Magna, Appl. Phys. Lett. **102**, 093101 (2013).
[53] I. Brihuega, E. Dupont-Ferrier, P. Mallet, L. Magaud, S. Pons, J. M. Gómez-Rodríguez, and J.-Y. Veuillen, Phys. Rev. B **72**, 205309 (2005).
[54] E. Dupont-Ferrier, P. Mallet, L. Magaud, and J.-Y. Veuillen, Phys. Rev. B **75**, 205315 (2007).
[55] Z. Y. Rong and P. Kuiper, Phys. Rev. B **48**, 17427 (1993).
[56] F. Varchon, P. Mallet, L. Magaud, and J.-Y. Veuillen, Phys. Rev. B **77**, 165415 (2008).
[57] I. Horcas, R. Fernández, J. M. Gómez-Rodríguez, J. Colchero, J. Gómez-Herrero, and A. M. Baro, Rev. Sci. Instrum. **78**, 013705 (2007).
[58] J. Ristein, S. Mammadov, and T. Seyller, Phys. Rev. Lett. **108**, 246104 (2012).
[59] H. Lüth, *Surface and Interfaces of Solid Materials*, 3rd ed. (Springer-Verlag, Berlin/Heidelberg, 1995).
[60] S. Mammadov *et al.*, 2D Mater. **1**, 035003 (2014).
[61] S. Shallcross, S. Sharma, and O. A. Pankratov, J. Phys.: Condens. Matter **20**, 454224 (2008).
[62] L. Xian, S. Barraza-Lopez, and M. Y. Chou, Phys. Rev. B **84**, 075425 (2011).
[63] K. Uchida, S. Furuya, J.-I. Iwata, and A. Oshiyama, Phys. Rev. B **90**, 155451 (2014).
[64] G. Trambly de Laissardière *et al.* (unpublished).
[65] E. Suárez Morell, P. Vargas, L. Chico, and L. Brey, Phys. Rev. B **84**, 195421 (2011).
[66] V. W. Brar, Y. Zhang, Y. Yayon, T. Ohta, J. L. McChesney, A. Bostwick, E. Rotenberg, K. Horn, and M. F. Crommie, Appl. Phys. Lett. **91**, 122102 (2007).
[67] Y. Zhang, V. W. Brar, F. Wang, C. Girit, Y. Yayon, M. Panlasigui, A. Zettl, and M. F. Crommie, Nat. Phys. **4**, 627 (2008).
[68] E. McCann, Phys. Rev. B **74**, 161403(R) (2006).